ELSEVIER

Applied Surface Science 127–129 (1998) 815–820

applied surface science

Sensitization of PMMA to laser ablation at 308 nm

R.L. Webb [a,1], S.C. Langford [a], J.T. Dickinson [a,*], T.K. Lippert [b]

[a] *Physics Department, Washington State University, Pullman, WA 99164-2814, USA*
[b] *Los Alamos National Laboratory, CST-6, MS J 585, Los Alamos, NM 87545, USA*

Abstract

Pure polymethylmethacrylate (PMMA) is highly resistant to ablation at 308 nm. The value of PMMA in lithography and semiconductor packaging and the availability of reliable 308 nm optics has motivated the development of dopants to facilitate PMMA ablation at 308 nm. We investigate the laser ablation of solvent cast PMMA films with and without pyrene, a typical dopant. The presence of residual solvent is shown to strongly promote laser ablation at low fluences in the case of chlorobenzene (CB), but not in the case of *N*-methyl 2-pyrrolidinone (NMP). At low laser fluences, many laser pulses may be required before significant neutral particle emissions are observed – an incubation effect. Scanning electron microscope observations indicate that the onset of emission coincides with the rupture of a thin surface layer, presumably depleted of solvent during film manufacture. The depleted layer would be relatively impervious to volatile fragments produced in the bulk. When this layer ruptures, volatile fragments escape and can be detected. Thus, the ablation behavior depends not only on the choice of dopant, but on the choice of solvent and the details of film manufacture. © 1998 Elsevier Science B.V.

PACS: 79.20Ds; 85.40Hp; 61.82.Pv

Keywords: PMMA; Laser ablation; Photo-resist

1. Introduction

Laser ablation of polymethylmethacrylate (PMMA) has been extensively studied due to its importance in lithography, semiconductor packaging, and medical applications [1–8]. Because of the unreliability of optical components in the far UV, 308 nm is the most convenient excimer wavelength for high through-put industrial applications. However, PMMA is essentially transparent at 308 nm, severely limiting applications at this wavelength. Therefore, most studies have been carried out at shorter excimer wavelengths.

Photochemically, UV laser radiation can photolyze the PMMA backbone chain, methyl side group, or ester side group [9,10]. At wavelengths longer than 230 nm, photolysis of the ester side group is, by far, the most important photolytic reaction. Each of these reactions yield small radicals, such as methoxy, methyl, and methylformate radicals, which can abstract hydrogen from the backbone to produce saturated products (CH_3OH, CH_4, $HCOOCH_3$). Abstraction can also conjugate bonds (forming C=C double bonds) along the backbone chain. Conjugated bond structures absorb strongly in the blue, giving irradiated PMMA a characteristic yellow appearance. As conjugated bonds accumulate, interactions in the

* Corresponding author. Tel.: +1-509-335-4914; fax: +1-509-335-7816; e-mail: jtd@wsu.edu.us.
[1] Current address: Physics Department, Pacific Union College, Angwin, CA 94508, USA.

0169-4332/98/$19.00 © 1998 Elsevier Science B.V. All rights reserved.
PII S0169-4332(97)00748-4

near UV are enhanced dramatically, resulting in pronounced 'incubation effects' [11–17]. Radical recombination with chain radicals can also initiate 'unzipping reactions' or 'depolymerization,' where successive chain scission events reduce the backbone to its constituent monomer units. Unless photolysis is very efficient, unzipping reactions can be responsible for the bulk of polymer decomposition during laser radiation.

In this paper, we re-examine the incubation process at 308 nm to clarify the role of absorbing dopants and a common solvent in the laser ablation of PMMA. We emphasize that our work is done at relatively low laser fluences, where polymer vaporization dominates material removal, as opposed to explosive fragmentation of the material [18,19]. The effect of laser radiation is studied by photo-absorption spectroscopy, quadrupole mass spectroscopy, time-of-flight techniques, and scanning electron microscopy. We show that occluded chlorobenzene (CB), a common PMMA solvent, is an effective sensitizer for vaporization at 308 nm.

2. Experiment

HPLC grade *N*-methyl 2-pyrrolidinone (NMP) and CB were alternatively used as solvents in the preparation of neat and pyrene-doped (0.1% by weight) PMMA samples. Medium molecular weight PMMA powder ($M_w = 120{,}000$) and pyrene chips (for pyrene-doped samples) were measured out by weight (typically 3 g combined mass) and poured into a flask containing 30 ml of solvent. This mixture was covered and stirred on low heat (50°C) for 6 h. The solution was then poured into a mold and held at 76°C for 12 h. The resulting films were typically 100–400-μm thick.

Laser irradiation was conducted in a diffusion-pumped, liquid-nitrogen trapped vacuum chamber at pressures below 10^{-5} Pa. The beam from a Lambda Physik, EMG 200 excimer laser with a 30-ns pulse length operating at 308 nm (XeCl) was directed onto the sample through a focusing lens (114-cm focal length) and mask. A low pulse repetition rate (1 Hz) was used to avoid cumulative heating in the sample. The fluence at the sample was controlled by adjusting the lens-to-sample distance. The total laser energy density per pulse (fluence) used in this work ranged from 0.1 to 5 J/cm^2.

Neutral emissions were studied with a UTI 100C quadrupole mass spectrometer (QMS) equipped with an electron impact ionizer operating at 70 eV. Ions formed in the ionizer were directed through the mass filter and detected with a Channeltron electron multiplier (CEM). The output of the CEM was directed into an electrometer, and the resulting amplified signal was digitized with a LeCroy 9450 digital oscilloscope.

3. Results

3.1. Absorption spectra

UV–VIS spectroscopy revealed distinctive features due to pyrene and chlorobenzene in those samples with these impurities, as shown in Fig. 1. Pyrene has a characteristic absorption band at 308 nm. CB-containing samples displayed absorption bands at ~300 and ~340 nm. These bands cannot be assigned to either PMMA *or* chlorobenzene alone, and may reflect polymer cage interactions [20]. These bands appreciably increase absorption at 308 nm. Although residual solvent concentrations were not determined in this work, we expect CB concentrations on the order of 20 wt% in our CB-cast PMMA. (Chlorobenzene concentrations below 20 wt% are difficult to attain in solvent cast PMMA [21].) Residual NMP in the NMP–PMMA samples showed no absorption features near 308 nm.

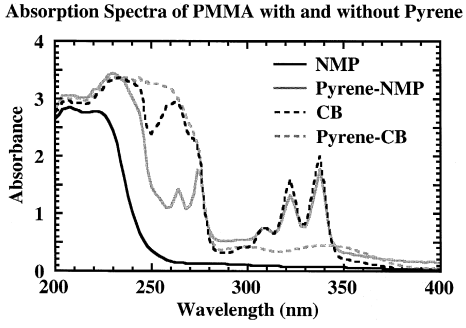

Fig. 1. The absorption spectra [$\log_{10}(I/I_0)$] of PMMA samples, including NMP–PMMA, Pyrene–NMP–PMMA, CB–PMMA, and Pyrene–CB–PMMA.

3.2. Neutral particle emission

The onset of neutral emission from cast PMMA does not exhibit a simple fluence threshold, but rather shows incubation behavior. Fig. 2 shows time-of-flight signals for 100 amu (the MMA monomer) recorded during the 10th, 19th, and 27th laser pulses on neat-CB material at a fluence of 0.9 J/cm^2. Prior to the onset of incubation (10th pulse), little, if any, emission is observed. During incubation (19th laser pulse), the emissions are weak, but fast, relative to subsequent emissions. Eventually, the emission intensities saturate at a relatively high value (27th laser pulse). As indicated in Fig. 2, the emission tends to slow down as the intensity saturates. Temperature estimates made by curve fitting half-range Maxwell–Boltzmann distributions to similar TOF curves suggest surface temperatures on the order of 1700 K near the onset of incubation, and on the order of 800 K near saturation. This effect is discussed below.

The course of incubation is readily evident when the peak intensity of the TOF peak is plotted on a pulse-to-pulse basis. The pulse-to-pulse evolution of the signal at 39 amu (an MMA fragment) for CB PMMA irradiated at 1.6 J/cm^2 is shown in Fig. 3. Little emission is observed until the onset of incubation, here at about 35 laser pulses. Despite the large pulse-to-pulse variations in intensity, the emission intensities clearly tend to saturate after 60 or 80 laser pulses. In situ measurements of the absorption at 308 nm for neat CB–PMMA and both pyrene doped materials show a strong increase in absorption during the initial stages of irradiation, which tends to saturate at about the same time the emission saturates.

The number of incubation pulses (N_i) required to initiate measurable neutral emission is a strong function of laser fluence and sample composition. The number of pulses required to initiate incubation at 100 amu was determined at several fluences for each

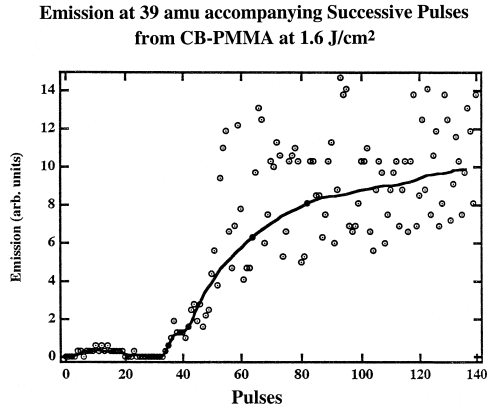

Fig. 3. The emission intensity of the 39 amu signal (primary cracking fraction of PMMA) accompanying consecutive laser pulses from CB–PMMA at a fluence of 1.6 J/cm^2.

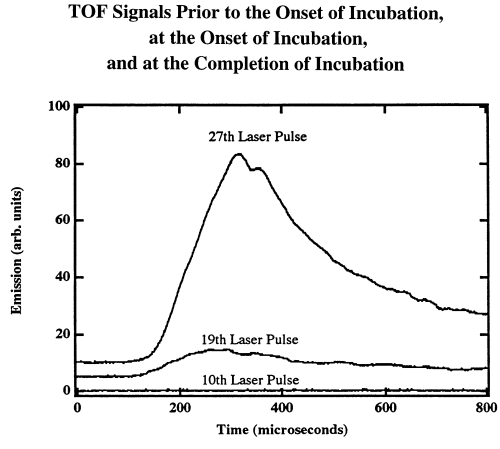

Fig. 2. The time-of-flight signals at 100 amu (MMA) taken before the onset of incubation, immediately the onset of incubation, and after the completion of incubation at 0.9 J/cm^2.

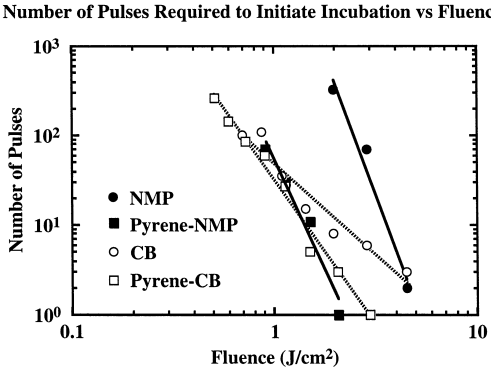

Fig. 4. The number of pulses required to initiate incubation vs. laser fluence for NMP–PMMA, Pyrene–NMP–PMMA, CB–PMMA, and Pyrene–CB–PMMA (log–log plot).

of four sample compositions and plotted in Fig. 4. As expected, the NMP-cast sample without pyrene requires many more pulses and/or higher fluences to induct than pyrene-doped NMP-case samples. Except that the very highest fluences, CB-cast samples without pyrene incubate much faster than NMP samples without pyrene. Significantly, the presence of pyrene does not significantly affect incubation in CB-cast samples at fluences below 1 J/cm^2; at higher fluences, pyrene accelerates the incubation process in CB-cast samples as well. The fluence/pulse number threshold for vaporization of PMMA is reduced considerably by the presence of either pyrene or chlorobenzene.

The effect of residual chlorobenzene on incubation was confirmed by comparing solvent-rich and solvent-poor samples, where the solvent concentration was varied by changing the duration and temperature of the anneal cycle after casting. Even in the presence of pyrene, high residual CB concentrations decreased the number of pulses required for incubation at 1.2 J/cm^2 from 46 to 26. Thus, enhanced residual CB concentrations reduce the 'dose' required for incubation at this fluence by almost a factor of two.

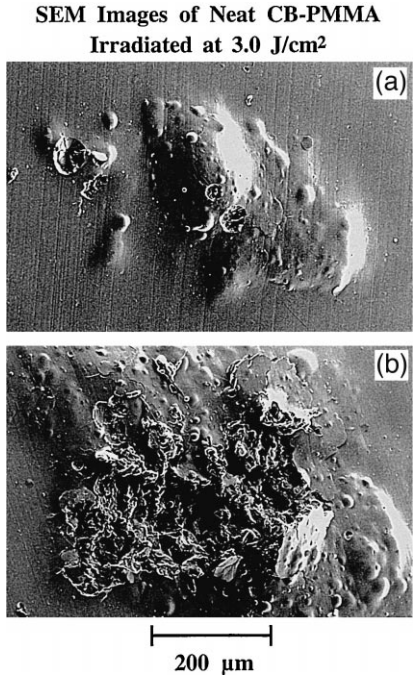

Fig. 5. The SEM images of CB–PMMA irradiated at 3.0 J/cm^2 after (a) two laser pulses (immediately after the onset of incubation) and (b) four laser pulses (incubation complete).

3.3. Surface evolution

The onset of incubation is accompanied by a marked change in the microscopic appearance of the samples. Scanning electron microscopy (SEM) images of CB-cast surfaces irradiated at 3.0 J/cm^2 are shown in Fig. 5, where irradiation was terminated at the onset of neutral emission in Fig. 5a (after two pulses) and after the saturation of neutral emission intensities in Fig. 5b (after four pulses). Immediately after the onset of incubation, the exposed surface shows localized cracks, consistent with rupture of a relatively impermeable 'skin' by gaseous products generated in the bulk. Relatively impermeable layers are often associated with solvent concentration gradients established by evaporation during fabrication. Since these solvents are effective plasticizers, material with high solvent concentrations (the bulk) is more flexible and permeable than material with low solvent concentrations (the surface layer). Volatile products created below the surface layer would then be trapped under the less permeable skin. After incubation is complete (emission saturates), the surface shows extensive cracking and melting.

The effect of the surface layer was confirmed by gently abrading the surface with 400 grit sandpaper; surface debris was removed with a jet of dry, clean air. Monomer neutral emission from abraded CB-cast material was observed at $\sim$0.2 J/cm^2 after 73 pulses. Induction in CB-cast material with an intact surface layer after 73 pulses requires about 0.9 J/cm^2 (from Fig. 4). SEM photographs of the abraded sample after incubation still show generalized swelling in the abraded region, which argues against scattering from scratches as a source of accelerated incubation. Interestingly, the abraded surface showed a uniform pattern of fine surface cracks after induction, suggesting that a weak surface layer (depleted in solvents) reformed after abrasion. The process of induction in this work (resulting in measurable neutral emission) is critically controlled by the breakup of the outer surface layer.

4. Discussion and conclusions

Combining the photochemical and thermal decomposition pathways, the following scenario can be posited. Photochemical reactions create many C=C double bonds, increasing UV absorption and enhancing further photochemical decomposition. Double bonds at chain ends also facilitate low activation energy thermal decomposition of PMMA. Since photochemical reactions can also be more efficient at higher temperatures [22], the elevated temperatures responsible for thermal decomposition can also accelerate photochemical decomposition. The combination of the two processes can function as a positive feedback system. Both photochemical and thermal reactions are important in this work, as revealed by the photo-yellowing of the sample, photoproducts (e.g., methylformate), the important thermal product MMA, and the temperatures derived from TOF measurements, which are consistent with thermal decomposition.

Chlorobenzene clearly enhances laser absorption, which would promote both photochemical and photothermal pathways. Further, photochemical dissociation of CB yields reactive chlorine radicals, [23] which are expected to abstract hydrogen from the polymer backbone. This will again produce C=C bonds and promote further photothermal interactions. At lower fluences, where the photochemical part of the CB interaction is especially effective in promoting decomposition, CB interactions dominate over pyrene-induced absorption.

Polyaromatic dopants, such as pyrene, are commonly employed with PMMA [24–28] and a general mechanism has been suggested for this class of dopants [29]. Pyrene principally promotes photothermal decomposition via cyclic photon absorption (often more than 10 photons during a laser pulse) [24], heating the matrix and promoting thermal decomposition of the polymer. At high fluences, efficient heating via cyclic photon absorption in pyrene strongly promotes rapid thermal decomposition and dominates over CB-induced effects.

The other important role of dopants and decomposition is the creation of small volatile molecules, which raise the internal pressure in polymer, eventually rupturing the thin ‘skin’ of solvent-depleted material that forms on solvent cast material. This skin typically prevents the detection of neutral products (methyl formate radical, solvent, or MMA) prior to the onset of incubation. With continued irradiation, the pressure exerted on the skin by accumulating volatile products ‘explosively’ ruptures the polymer, allowing decomposition products to escape and producing the distinct crack-like features on the polymer surface.

Acknowledgements

We thank Charles Davis, IBM–Endicot, for helpful discussions. This work was supported by IBM and the Department of Energy, Office of Basic Energy Sciences, Division of Chemical Sciences under Contracts DE-FG06-92ER14252, and DE-FG07-97ER62516.

References

[1] P.E. Dyer, in: I.W. Boyd, R.B. Jackman (Eds.), Photochemical Processing of Electronic Materials, Academic Press, London, 1992, p. 359.
[2] M. Isner, P.G. Steg, R.H. Clarke, IEEE J. Quantum Electron. QE 23 (1986) 482.
[3] R. Iscoff, Laser and Optronics 6 (1987) 65.
[4] R.J. Lane, R. Linsker, J.J. Wynne, A. Torres, R.G. Geronemus, Arch. Dermatol. 121 (1985) 609.
[5] H. Nornes, R. Srinivasan, R. Solanski, E. Johnson, Soc. Neurosci. 11 (1985) 1167.
[6] S. Lazare, V. Granier, Laser Chem. 10 (1989) 25.
[7] Y.T.C. Yeh, J. Vac. Sci. Technol. A 4 (1986) 653.
[8] R. Srinivasan, B. Braren, Chem. Rev. 89 (1989) 1303.
[9] J.F. McKellar, N.S. Allen, Photochemistry of man-made polymers, Appl. Science, 1979, p. 89.
[10] A. Gupta, R. Liang, F.D. Tsay, J. Moacanin, Macromolecules 13 (1980) 1696.
[11] R. Srinivasan, B. Braren, K.G. Casey, Pure Appl. Chem. 62 (1990) 1581.
[12] G.M. Davis, M.C. Gower, J. Appl. Phys. 61 (1987) 2090.
[13] A.K. Baker, P.E. Dyer, Appl. Phys. A 57 (1993) 543.
[14] J. Meyer, J. Kutzner, D. Feldmann, K.H. Welge, Appl. Phys. B 45 (1988) 7.
[15] S. Küper, M. Stuke, Appl. Phys. A 49 (1989) 211.
[16] S. Lazare, J. Lopez, J.-M. Turlet, M. Kufner, S. Kufner, P. Chavel, Appl. Opt. 35 (1996) 4471.
[17] R. Srinivasan, B. Braren, K.G. Casey, J. Appl. Phys. 68 (1990) 1842.
[18] T. Lippert, J. Stebani, J. Ihlemann, O. Nuyken, A. Wokaun, Angew. Makromol. Chem. 213 (1993) 127.

[19] T. Lippert, J. Dauth, O. Nuyken, A. Wokaun, in: J.J. Pireaux, P. Bertrand, J.L. Bredas (Eds.), Polymer–Solid Interfaces, Institute of Physics, Bristol, 1992, p. 391.
[20] A.C. Ouano, R. Pecora, Macromolecules 13 (1980) 1173.
[21] A.C. Ouano, R. Pecora, Macromolecules 13 (1980) 1167.
[22] J.L. Graham, J.M. Berman, B. Dellinger, J. Photochem. Photobiol. A Chem. 71 (1993) 65.
[23] A. Tissot, P. Boule, J. Lemaire, Chemosphere 13 (1984) 382.
[24] H. Fujiwara, H. Fukumura, H. Masuhara, J. Phys. Chem. 99 (1995) 11844.
[25] H. Masuhara, H. Hiraoka, K. Domen, Macromolecules 20 (1987) 450.
[26] H. Hiraoka, T.J. Chuang, H. Masuhara, J. Vac. Sci. Technol. B 6 (1988) 463.
[27] T.J. Chuang, H. Hiraoka, A. Mödl, Appl. Phys. A 45 (1988) 277.
[28] A. Itaya, A. Kurahashi, H. Masuhara, Y. Tanaguchi, M. Kiguchi, J. Appl. Phys. 67 (1990) 2240.
[29] H. Fukumura, H. Masuhara, Chem. Phys. Lett. 221 (1994) 373.